

# Investigation of the magnetic field of the permanent magnet applied in the DIRAC experiment

P. Batyuk<sup>a</sup>, O. Gortchakov<sup>a</sup>, V. Yazkov<sup>b</sup>

June 1, 2012

## Abstract

An analysis of the experimental data obtained during the run of 2011 has revealed the effect of degradation of the permanent magnet used. This effect is investigated, and average magnetic field is estimated for each day of the run.

## Introduction

The main purpose of the 2011 run is a search of pion atoms in a metastable state. To achieve this goal, it is very important to analyse the transverse momenta  $Q_y$  of  $\pi^+\pi^-$  pairs.

Fig. 1 shows that the peak in the distribution of experimental events over  $Q_y$  is shifted with respect to the same peak for simulated events. This shift may be explained by degradation of the permanent magnet situated downstream of the Be target. The following situation occurred several times during the run: elements of the experimental setup, including, also, the magnet, were hit by the incident beam. With time, the energy of atomic nuclei released in transitions from excited to lower states could lead to an increase in the temperature of certain magnet domains up to values exceeding the Curie temperature, which on the whole would result in a decrease of the magnetic field of the permanent magnet. And even at normal beam condition magnet is hit by secondary high energy particles which also could provide demagnetization of the permanent magnet.

This paper presents a quantitative description of the magnet degradation. An attempt to determine the average magnetic field corresponding to each day of the run has been made.

To resolve the problem, analysis of the transverse momentum  $Q_y$  of  $e^+e^-$  pairs from conversion of the  $\gamma$ -quanta was carried out. The choice of  $e^+e^-$  pairs for the analysis is explained by the fact that in this case quantitative description of the magnet degradation can be performed with higher accuracy (due to the narrower peak we are interested in, as one can see from Fig. 2, comparing it with Fig. 1).

As it can be seen from Figs. 3 and 4, the leftward shift of the peak of interest is also evident in the case of  $e^+e^-$  pairs from  $\gamma$  conversion.

---

<sup>a</sup>Joint Institute for Nuclear Research, Russia

<sup>b</sup>Skobeltsin Institute of Nuclear Physics, Lomonosov Moscow State University, Russia

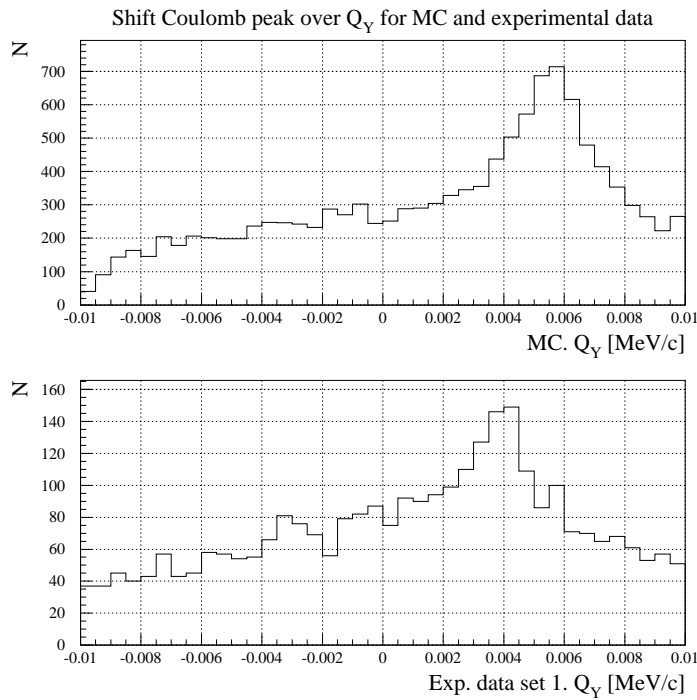


Figure 1: Simulated (upper) and experimental (lower) distributions of  $\pi^+\pi^-$  pairs over  $Q_y$ . Statistics have been collected during the period from June 25 up to July 1.

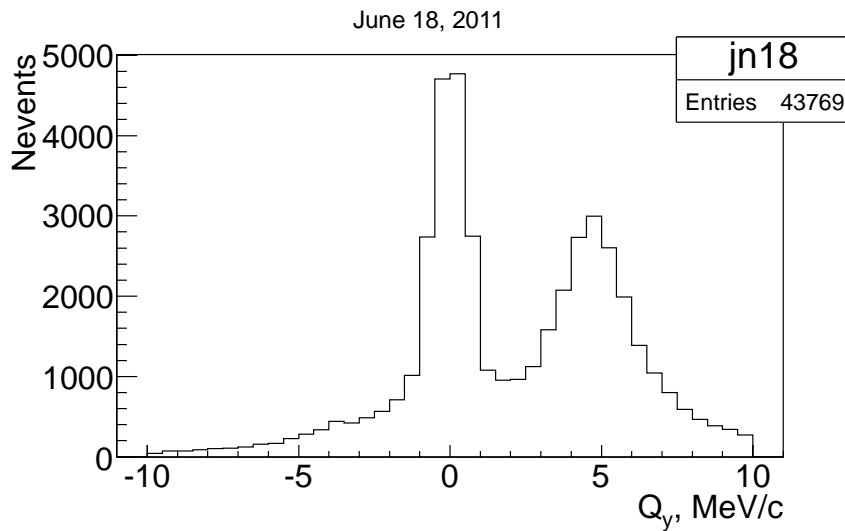


Figure 2: Example of experimental distribution over  $Q_y$  for  $e^+e^-$  pairs from  $\gamma$  conversion.

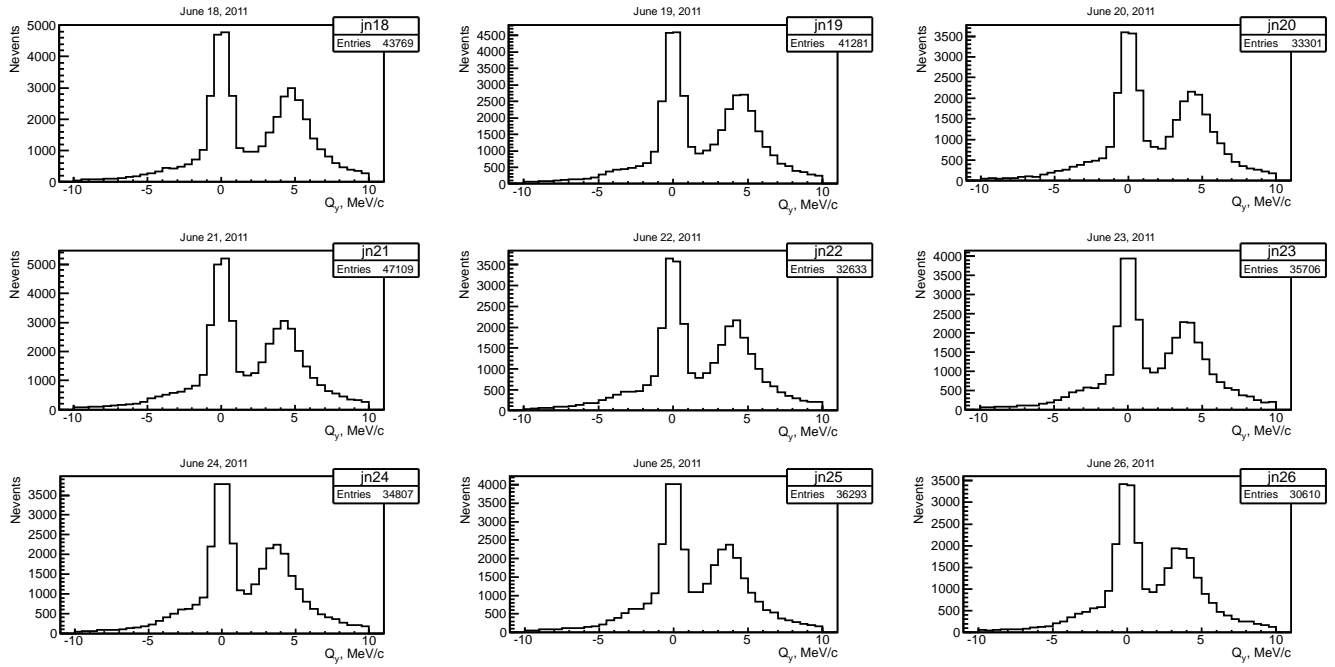


Figure 3: Experimental distribution of  $e^+e^-$  pairs from  $\gamma$  conversion over  $Q_y$  for several days of the 2011 run.

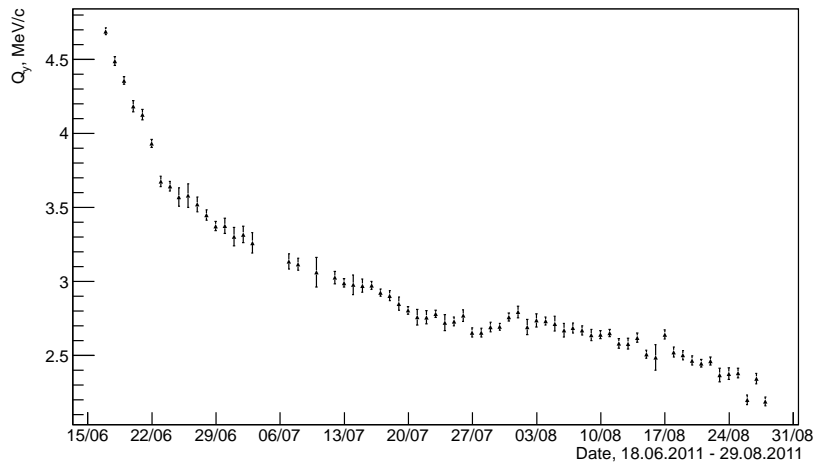


Figure 4: Position of shifted peak in the distribution over  $Q_y$  as function of day of the run (data are presented for the first half of the run).

It should be taken into account, that the  $e^+e^-$ -pairs could be the following:

1. pairs, produced as a result of the conversion of  $\gamma$ -quanta in the Be target;
2. pairs, resulting from internal conversion in the Be target  $\pi^0 \rightarrow \gamma e^+e^-$  (i.e. Dalitz pairs);
3. pairs, produced in the conversion of  $\gamma$ -quanta in platinum foil, mylar, air, the fiber and other detectors.

$e^+e^-$  pairs from conversion (including internal conversion) in the target form the shifted peak, all other pairs contribute to the peak near zero. This is due to the target being situated before the permanent magnet, the magnetic field of which deflects electrons and positrons from  $e^+e^-$  pairs produced in the Be target.

## Algorithm and procedure for estimation of the magnetic field

First, the interval of magnetic field values  $(0.0 \dots 1.0)$ <sup>1</sup> was divided into 40 intervals with bins of 0.025.

The **first step** consisted in applying the GEANT-DIRAC program [1] for simulation of events of  $\gamma$  conversion into  $e^+e^-$  pairs (Dalitz pairs were also taken into account) within and after the Be target for each value of the magnetic field. It is also very important, that the simulated events contain information on the z-coordinate of the conversion point permitting determination of whether the conversion took place before or after the permanent magnet.

The simulated data were further transferred to the reconstruction program ARIANE, the output of which was recorded in Ntuple's of the form standard for the DIRAC experiment. The Ntuple's were subsequently transformed into ROOT-trees.

At the **second step**, the experimental events for each day (18.06.2011 - 15.11.2011) were fitted by the sum of two simulated distributions (for conversion within and after the Be target, respectively) for each value of the magnetic field (0.0, 0.025, 0.050 ... 0.950, 0.975, 1.0), upon which distributions were constructed demonstrating the dependence of the  $\chi^2$  values upon the magnetic field; such dependences are shown in Fig. 5 for several days of the run. From fits obtained for each day, only the one, providing the minimum  $\chi_{min}^2$  value, was finally chosen, so as to extract the value  $H_{min}$  corresponding to this fit.

Further, distributions for each day, similar to the distributions in Fig. 5, were fitted by second order polynomials (red line in Fig. 5) within the interval  $(H_{min} - \delta, H_{min} + \delta)$ , where  $\delta = 0.075$ . The value  $H_{min}^{fit}$  determined by the minimum of a parabolic fit was considered the averaged value of the magnetic field for each day of the run.

At the **third step** errors were estimated for the reconstructed value  $H_{min}^{fit}$  of the magnetic field. This was done in the following way. We took the  $\chi^2$  value, differing from the minimum value  $\chi_{min}^2$ , by unity (i.e.  $\chi^2 = \chi_{min}^2 + 1$ ), and, using the parameters of the parabolic fit that yielded  $H_{min}^{fit}$ , we obtained two values  $H_{left}^{fit}$  and  $H_{right}^{fit}$  ( $H_{left}^{fit} < H_{min}^{fit} < H_{right}^{fit}$ ) by resolving the corresponding quadratic equation.

---

<sup>1</sup>The value 1.0 corresponds to the initial magnetic field of the magnet, and 0.0 corresponds to the case when no magnetic field is present.

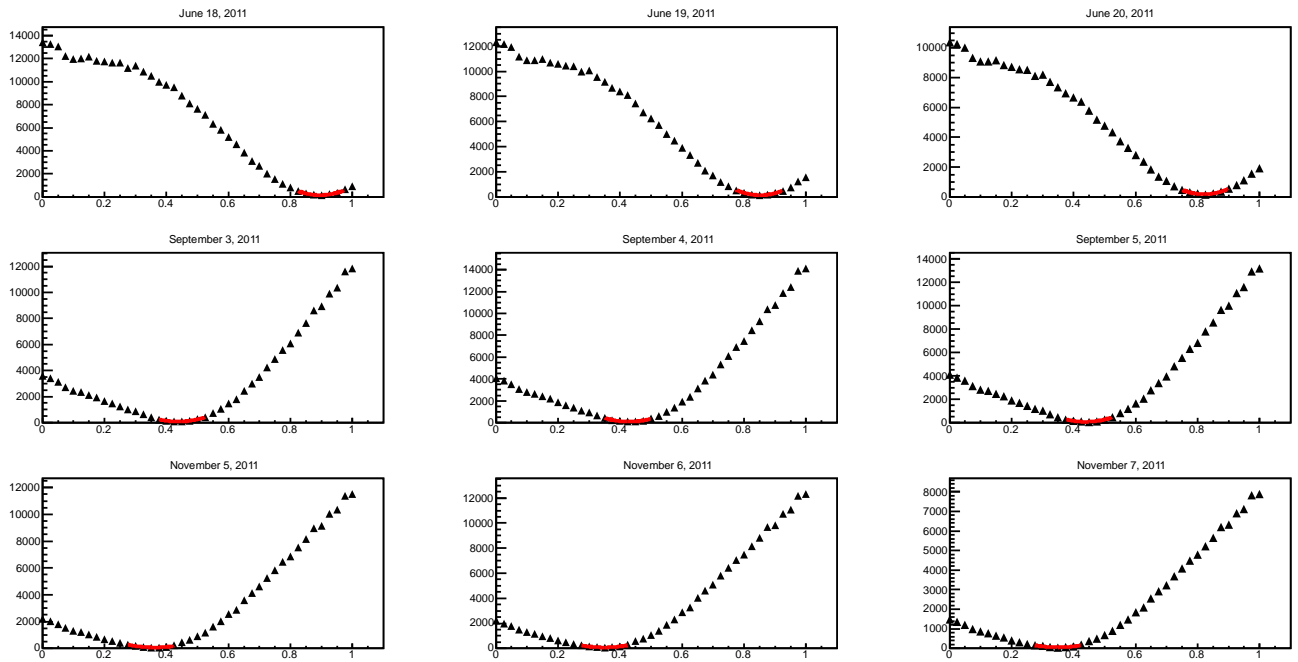


Figure 5: Dependence of values  $\chi^2$  values upon the magnetic field for separate days of the run.

As an estimate for the uncertainty in the daily magnetic field we adopted the value

$$\Delta H_{min}^{fit} = \frac{H_{right}^{fit} - H_{left}^{fit}}{2}$$

The results obtained are presented in Fig. 6 and Tab. 1.

## Conclusion

The sharp decrease in the magnetic field corresponding to June 22 - June 23 and November 8 - November 9 (see Fig. 6), could be explained by a strong irradiation of the construction elements of the experimental setup, including the magnet (see above). The slight bump near August 1 (see also Fig. 4) is related to a change in the position of the magnet realized in order to focus the secondary beam in the center of the magnetic field. The drop at the end of the run may be explained by certain problems that occurred at the time with the accelerator.

Table 1: Number of events, value of magnetic field and error in magnetic field for each day of the run of 2011.

Date	N <sub>events</sub>	$H_{min}^{fit} \pm \Delta H_{min}^{fit}$	Date	N <sub>events</sub>	$H_{min}^{fit} \pm \Delta H_{min}^{fit}$
June 18	43769	$0.895 \pm 0.004$	September 3	40680	$0.437 \pm 0.005$
June 19	41281	$0.853 \pm 0.004$	September 4	54222	$0.429 \pm 0.004$
June 20	33301	$0.821 \pm 0.004$	September 5	48757	$0.439 \pm 0.004$
June 21	47109	$0.793 \pm 0.004$	September 6	56682	$0.428 \pm 0.004$

Table 1: Number of events, value of magnetic field and error in magnetic field for each day of the run of 2011.

Date	N <sub>events</sub>	$H_{\min}^{\text{fit}} \pm \Delta H_{\min}^{\text{fit}}$	Date	N <sub>events</sub>	$H_{\min}^{\text{fit}} \pm \Delta H_{\min}^{\text{fit}}$
June 22	32633	$0.784 \pm 0.004$	September 7	49614	$0.428 \pm 0.004$
June 23	35706	$0.747 \pm 0.004$	September 8	61810	$0.425 \pm 0.004$
June 24	34807	$0.699 \pm 0.004$	September 9	47201	$0.419 \pm 0.005$
June 25	36293	$0.685 \pm 0.004$	September 10	54305	$0.421 \pm 0.004$
June 26	30610	$0.685 \pm 0.004$	September 11	14166	$0.42 \pm 0.01$
June 27	15841	$0.68 \pm 0.01$	September 12	33061	$0.420 \pm 0.005$
June 28	27416	$0.665 \pm 0.005$	September 13	30619	$0.413 \pm 0.005$
June 29	32508	$0.661 \pm 0.005$	September 14	58493	$0.419 \pm 0.004$
June 30	34446	$0.646 \pm 0.004$	September 15	45344	$0.410 \pm 0.005$
July 1	19946	$0.64 \pm 0.01$	September 16	48383	$0.406 \pm 0.004$
July 2	21305	$0.63 \pm 0.01$	September 17	55107	$0.416 \pm 0.004$
July 3	19217	$0.63 \pm 0.01$	September 18	48473	$0.402 \pm 0.004$
July 4	13739	$0.61 \pm 0.01$	September 19	44334	$0.404 \pm 0.004$
July 7	7668	$0.61 \pm 0.01$	September 20	53151	$0.403 \pm 0.004$
July 8	15806	$0.60 \pm 0.01$	September 21	57893	$0.401 \pm 0.004$
July 9	18784	$0.591 \pm 0.005$	September 22	24150	$0.405 \pm 0.005$
July 10	7091	$0.59 \pm 0.01$	September 23	43982	$0.399 \pm 0.004$
July 11	2428	$0.58 \pm 0.01$	September 24	38801	$0.400 \pm 0.005$
July 12	15451	$0.57 \pm 0.01$	September 25	61149	$0.390 \pm 0.004$
July 13	24005	$0.574 \pm 0.005$	September 26	49011	$0.396 \pm 0.004$
July 14	31916	$0.573 \pm 0.004$	September 27	56301	$0.391 \pm 0.004$
July 15	18498	$0.573 \pm 0.005$	September 28	32316	$0.391 \pm 0.005$
July 16	27184	$0.566 \pm 0.005$	September 29	43304	$0.392 \pm 0.005$
July 17	43128	$0.563 \pm 0.004$	September 30	55305	$0.393 \pm 0.004$
July 18	46709	$0.557 \pm 0.004$	October 1	63972	$0.388 \pm 0.004$
July 19	43631	$0.557 \pm 0.004$	October 2	53564	$0.389 \pm 0.004$
July 20	38956	$0.546 \pm 0.004$	October 3	59152	$0.385 \pm 0.004$
July 21	44630	$0.536 \pm 0.004$	October 4	58661	$0.384 \pm 0.004$
July 22	37116	$0.531 \pm 0.004$	October 5	62475	$0.385 \pm 0.004$
July 23	47070	$0.523 \pm 0.004$	October 6	52749	$0.384 \pm 0.004$
July 24	46068	$0.524 \pm 0.004$	October 7	44098	$0.385 \pm 0.004$
July 25	38797	$0.520 \pm 0.004$	October 8	65514	$0.377 \pm 0.004$
July 26	39968	$0.519 \pm 0.004$	October 9	63661	$0.384 \pm 0.004$
July 27	19393	$0.52 \pm 0.01$	October 10	59388	$0.382 \pm 0.004$
July 28	49750	$0.505 \pm 0.004$	October 11	38270	$0.373 \pm 0.005$
July 29	42739	$0.503 \pm 0.004$	October 12	35008	$0.377 \pm 0.005$
July 30	35993	$0.503 \pm 0.005$	October 13	59095	$0.376 \pm 0.004$
July 31	45581	$0.506 \pm 0.004$	October 14	29622	$0.379 \pm 0.005$
August 1	51263	$0.517 \pm 0.004$	October 15	62042	$0.369 \pm 0.004$

Table 1: Number of events, value of magnetic field and error in magnetic field for each day of the run of 2011.

Date	$N_{\text{events}}$	$H_{\text{min}}^{\text{fit}} \pm \Delta H_{\text{min}}^{\text{fit}}$	Date	$N_{\text{events}}$	$H_{\text{min}}^{\text{fit}} \pm \Delta H_{\text{min}}^{\text{fit}}$
August 2	59517	$0.524 \pm 0.004$	October 16	59815	$0.368 \pm 0.004$
August 3	52725	$0.516 \pm 0.004$	October 17	54442	$0.372 \pm 0.004$
August 4	19327	$0.52 \pm 0.01$	October 18	51499	$0.371 \pm 0.004$
August 5	45917	$0.515 \pm 0.004$	October 19	59203	$0.367 \pm 0.004$
August 6	48639	$0.514 \pm 0.004$	October 20	54824	$0.368 \pm 0.004$
August 7	31205	$0.508 \pm 0.005$	October 21	50171	$0.367 \pm 0.004$
August 8	42419	$0.513 \pm 0.004$	October 22	59366	$0.364 \pm 0.004$
August 9	35291	$0.504 \pm 0.004$	October 23	58346	$0.363 \pm 0.004$
August 10	32966	$0.505 \pm 0.005$	October 24	48948	$0.36 \pm 0.01$
August 11	52049	$0.498 \pm 0.004$	October 25	48082	$0.37 \pm 0.01$
August 12	53174	$0.500 \pm 0.004$	October 26	12604	$0.35 \pm 0.01$
August 13	56859	$0.492 \pm 0.004$	October 27	37250	$0.36 \pm 0.01$
August 14	37390	$0.489 \pm 0.004$	October 28	40099	$0.35 \pm 0.01$
August 15	50021	$0.490 \pm 0.004$	October 29	15547	$0.35 \pm 0.01$
August 16	35974	$0.485 \pm 0.004$	October 30	30437	$0.36 \pm 0.01$
August 17	31736	$0.481 \pm 0.005$	October 31	24872	$0.36 \pm 0.01$
August 18	29049	$0.485 \pm 0.005$	November 1	35027	$0.35 \pm 0.01$
August 19	42461	$0.481 \pm 0.004$	November 2	32495	$0.35 \pm 0.01$
August 20	63908	$0.472 \pm 0.004$	November 3	38996	$0.36 \pm 0.01$
August 21	64515	$0.475 \pm 0.004$	November 4	40277	$0.35 \pm 0.01$
August 22	65075	$0.471 \pm 0.004$	November 5	32953	$0.36 \pm 0.01$
August 23	65130	$0.467 \pm 0.004$	November 6	33683	$0.35 \pm 0.01$
August 24	51988	$0.459 \pm 0.004$	November 7	17492	$0.35 \pm 0.01$
August 25	53698	$0.464 \pm 0.004$	November 9	18353	$0.34 \pm 0.01$
August 26	52902	$0.456 \pm 0.004$	November 10	33248	$0.30 \pm 0.01$
August 27	66916	$0.445 \pm 0.004$	November 11	33248	$0.30 \pm 0.01$
August 28	62714	$0.448 \pm 0.004$	November 14	7337	$0.13 \pm 0.01$
August 29	61568	$0.441 \pm 0.004$	November 15	12759	$0.11 \pm 0.01$
$N_{\text{total}} = 5896101$					

Fig. 7 presents the number of experimental events for each day of the run; Fig. 8 and Table 2 show the number and fraction of events corresponding to the magnetic field  $H_{\text{min}}$ .

## References

- [1] DIRAC-NOTE-2012-01: The generator of photons in the reaction  $p + Ni \rightarrow \gamma + X$  at 24 GeV/c, O. Gortchakov [JINR].

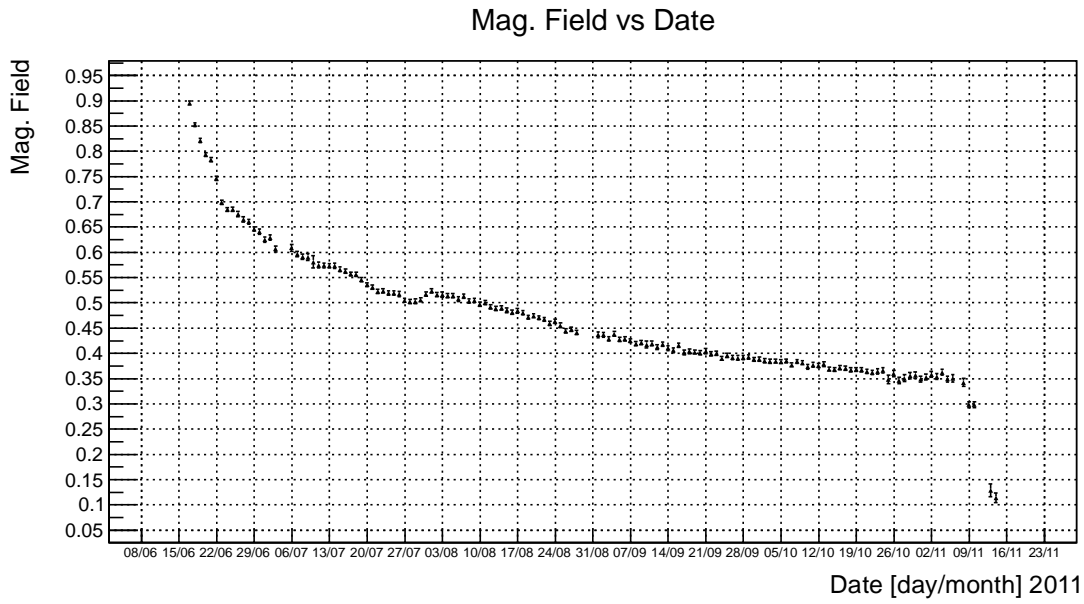


Figure 6: Average value of magnetic field for each day of the run.

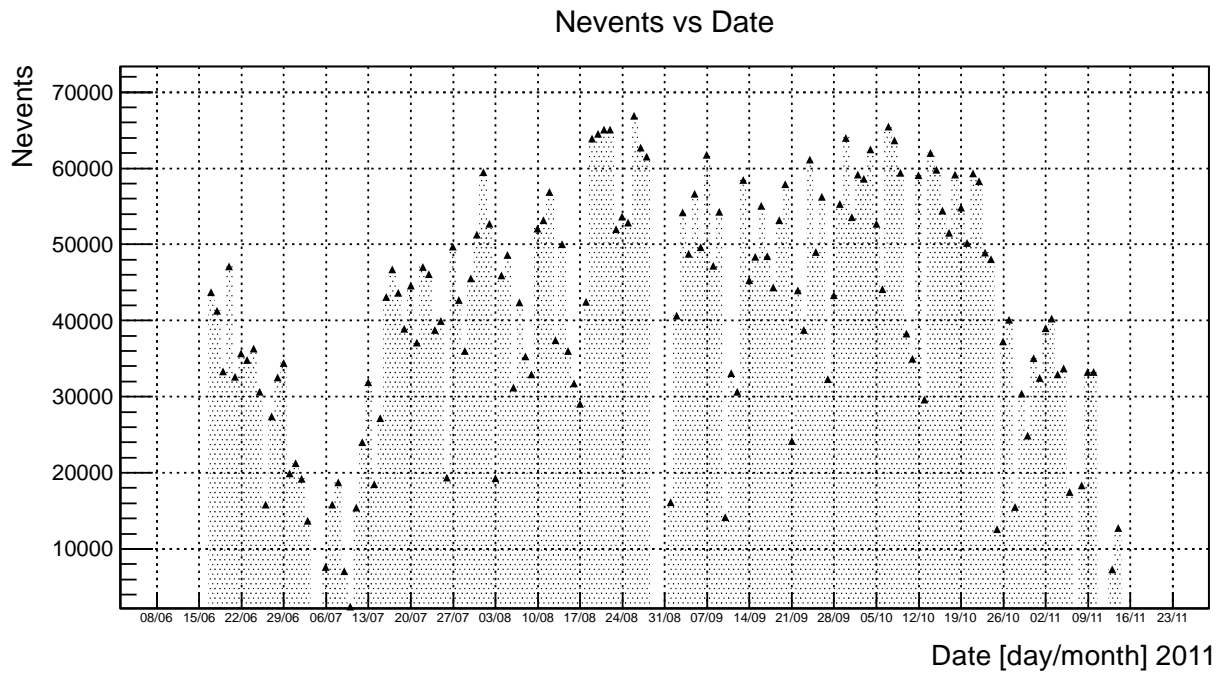


Figure 7: Number of experimental events for each day of the run.



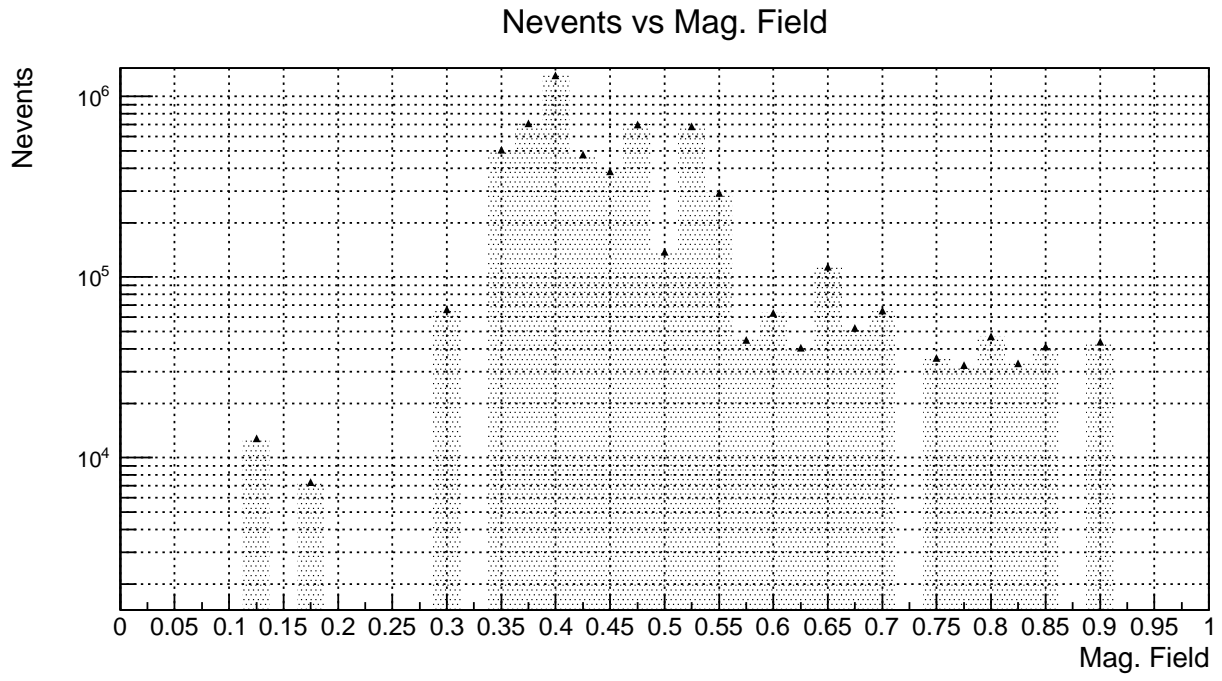


Figure 8: Number of events corresponding to magnetic field  $H_{min}$ .

Table 2: Number and fraction of experimental events corresponding to discrete value  $H_{min}$ .

$H_{min}$	$N_{events}$	$\eta, \%$	$H_{min}$	$N_{events}$	$\eta, \%$
0.025	0	0	0.525	683674	11.60
0.050	0	0	0.550	291605	4.95
0.075	0	0	0.575	44931	0.76
0.100	0	0	0.600	63088	1.07
0.125	12759	0.22	0.625	40522	0.69
0.150	0	0	0.650	114316	1.94
0.175	7337	0.12	0.675	52134	0.88
0.200	0	0	0.700	65417	1.11
0.225	0	0	0.725	0	0
0.250	0	0	0.750	35706	0.61
0.275	0	0	0.775	32633	0.55
0.300	66496	1.13	0.800	47109	0.80
0.325	0	0	0.825	33301	0.56
0.350	507115	8.60	0.850	41281	0.70
0.375	707595	12.00	0.875	0	0
0.400	1304350	22.12	0.900	43769	0.74
0.425	476333	8.08	0.925	0	0
0.450	385525	6.54	0.950	0	0
0.475	701039	11.89	0.975	0	0
0.500	138070	2.34	1.000	0	0